

# Worm Robot with Dynamic Adaptation to Pipe Diameter for In-Pipe Inspection<sup>1</sup>

<sup>1</sup>Basem F. Yousef<sup>†</sup> and <sup>2</sup>Nabil Bastaki

<sup>1</sup>Mechanical Engineering, United Arab Emirates University, basem\_yousef@uaeu.ac.ae

<sup>2</sup>Electrical Engineering, United Arab Emirates University, nabil@uaeu.ac.ae

**Abstract**— *This paper proposes an in-pipe inspection robot that can adapt to changes in pipe diameter. The sophisticated design and configuration of the robot enables it to travel autonomously through pipes and adapt to diameters changing from 65mm to 220mm. It consists of two clamping modules and one module for steering and locomotion. The clamping modules utilize flexible spring sheets to enable the robot to dynamically adjust its radial dimension and clamping force to attach to pipes of different inner diameters and handle sudden or smooth changes in pipe diameters. A middle module is engineered to enable the robot to not only propel through the pipeline, but also to steer into the desired direction when approaching elbows or junctions. The robot finds its obstacle-free path using a set of sensors mounted on the robot nose.*

**Index Terms**—Autonomous robot, adaptation to pipe diameter, pipeline inspection, steering.

## I. INTRODUCTION

Pipelines are extensively used to carry natural gas and oil to destinations throughout the world. They range from high-pressure transmission lines to low-pressure distribution lines. In order to prevent a failure/leakage in a pipeline due to corrosion and/or high pressure, the interiors of the pipes need to be routinely monitored and inspected to evaluate the need to maintain or repair the pipeline, and to decide the most effective means of doing so. Although cutting one or more samples of the pipe is one of the most common methods used for diagnosing a pipeline, its main disadvantage is attributed to the high cost and downtime associated with the method, other than the fact that this method does not provide a comprehensive picture about the status of the whole pipe because of the variations in corrosion rate or deposit buildup found in different sections of a pipe. Moreover, many pipes are located either underground or under water, or even in places difficult to access. Therefore, many concepts of Pipe Inspection Robots (PIR) have been utilized as alternative methods [1-24] to access pipes from inside.

\* This work was supported by Research Affairs at the United Arab Emirates University under Research Grant # 1605-07-01-10 (PI: Basem F. Yousef). Features of the design are reported and claimed in US provisional patent file No. 61577020.

<sup>†</sup> Basem F. Yousef. Tel.: +971-50-1121 683; fax: +971-3-762 3158. [basem\\_yousef@uaeu.ac.ae](mailto:basem_yousef@uaeu.ac.ae).

Since space availability is one of the challenges that face in-pipe robots[1], many concepts have been adopted to tackle this challenge and resulted in developing different kinds of in-pipe robots such as pig type, wheel type, caterpillar type, wall-press type, walking type, inchworm type and screw types, and the development of other robots that adopt combinations of those concepts [1-24]. Moreover, pipe radii vary by the usage and flow conditions of the pipes, hence another main challenge that may pose technical difficulties to PIRs is the ability to navigate inside a pipe of changing diameter e.g. a pipe comprising segments of different diameters. This challenge becomes more difficult when the change in pipe diameter is 1) in step (not smooth) and; 2) the diameter change is considerably large e.g., more than double the smaller section. In these scenarios, when the robot passes from a larger pipe to a smaller pipe diameter, it has to be able to: a) find the hole location at the cross-section where the pipes mate (e.g. up, down, right or left of the center of the hosting pipe segment); b) steer into the hole direction; c) change its radial dimension to negotiate the receiving pipe diameter; and d) propel/move autonomously forward and backward in a limited and constrained space.

Several concepts of PIRs have been developed to move through a pipeline [2-7] with propulsion mechanisms that depend on friction force which may not be always sufficient to cause the motion. Other mechanisms were designed to overcome those difficulties by utilizing sets of front and rear rollers/wheels which are pushed against the interior wall of the pipe and used to drive the robot [8-13]. Although some of those PIRs could travel only in pipes of constant diameters [8,9], others could handle only small changes in pipe diameters since their wheels are pushed radially against the pipe walls using compression springs of small strokes. Also their springs usually exert smaller forces towards the end of the spring stroke causing slipping of the wheels [10-15]. one notable example on a PIR that can adapt to large changes in pipe diameters is [13], which could handle a pipe change of 400-700 mm. It uses 3 pantograph mechanisms distributed radially at 120 degrees to push the wheels against the pipe

walls, thus belongs to the wheel-driven robots. Its configuration allows to maintain 3 contact points between the wall and each of the 3 the drive mechanisms. However, the contact points location pose constraints on the length of the robot and its diameter, and it may cause collisions when passing through pipe of large diameter to a smaller one through a step connection.

Moreover, inch-worm robots [16-18] and snake-like robots [19-21] utilize a serpentine motion to travel through horizontal and curved pipes, but their designs allow for

limited radial and axial extension-contraction to provide clamping force against pipe walls. Also, pipe crawlers demonstrated good ability in dealing with the change in pipe diameters [22, 23]. In spite of the advanced designs of those robots, their intricate designs showed deficiencies in meeting one or more of the intended tasks when navigating through a pipeline especially when dealing with sudden changes in pipe diameter.

In addition, magnetic wheels were utilized in [24] to provide a wall climbing robot that may be used for inspecting the interior of surfaces of gas-tanks in oversea ships, however it lacks the ability to adapt to pipe diameter and it is material dependent.

In this paper, we continue the effort of designing a sophisticated engineering solution of a pipe inspection robot that can efficiently adapt to changes of pipe diameter, whether step or smooth, and to pass easily through elbows. The initial conceptual design was reported in [25]. The novel design of the proposed robot adopts an inchworm locomotion concept to navigate autonomously through a pipeline. Detailed description, performance analysis and testing is explained in the subsequent sections.

## II. ROBOT DESCRIPTION

The robot consists of three main segments, two identical end clamps and a middle segment, in addition to a sensor assembly to enable the path-realizing feature. The clamps enable the robot to firmly attach to the inner walls of the pipe exerting a preset constant clamping force in both straight pipe segments and in elbows regardless of the diameter of the pipe or elbow, while the middle segment provides means to a) move and to b) steer the robot inside elbows or into the direction of a clear path, as explained later. (Figs. 1 and 2). The modules are connected by two ball joints to provide flexibility needed to allow the robot to pass through turns. All batteries and control drives are kept in a special compartment connected to the middle segment.

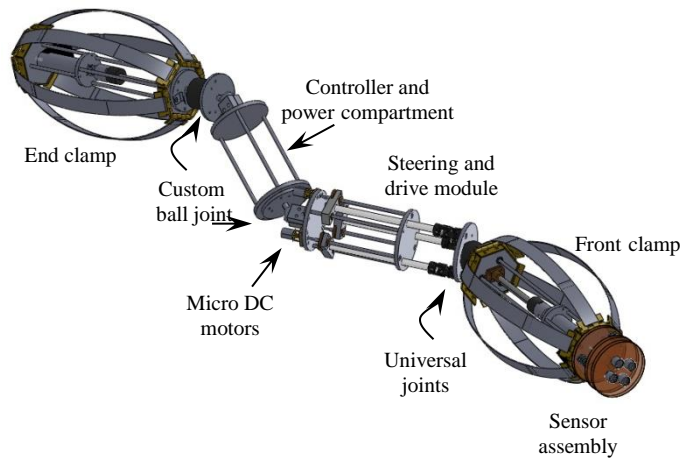


Fig. 1. A 3D CAD model of the robot showing the different modules

### A. The Clamps

The main function of the clamps (Fig. 3a) is to provide temporary contact with the inner walls of the pipe. Each clamp assembly is built around a motor and consists of 6 flexible spring sheets connected at their ends to hexagonal flanges by hinges. The flanges are connected with a power screw and a DC motor which both are aligned to form the clamp's axis. While one hexagonal flange is fixed at the end of the clamp, the other flange slides along the power screw when the motor rotates. This movement causes the flexible spring sheets to straighten or bend outwards to change the radial dimension of the clamp, thus causing the sheets to come in contact with the inner wall of the pipe. The closer the flanges are, the wider the opening of the spring sheets is and hence, the stronger the clamping force to the pipe will be (Fig. 3b).

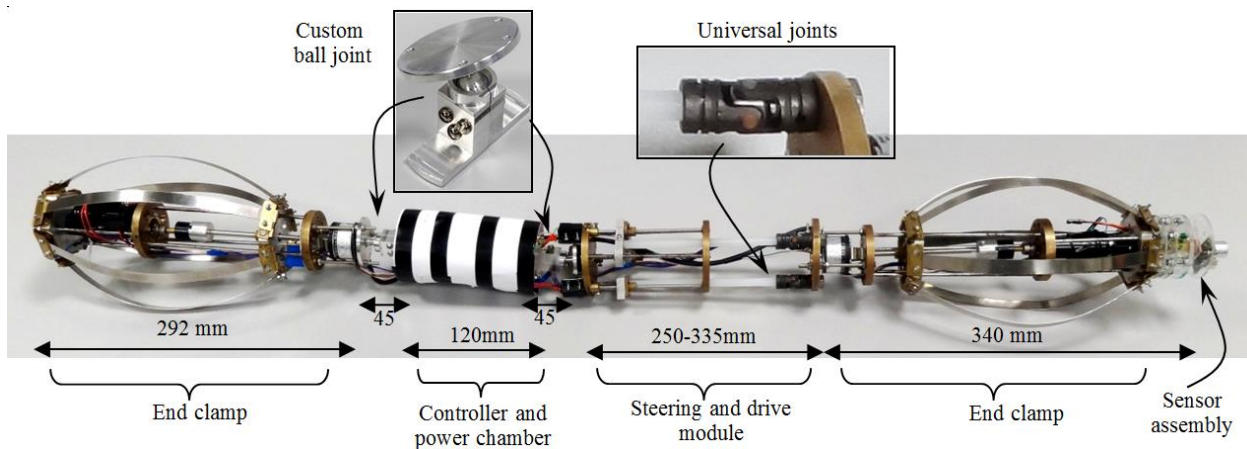


Fig. 2. Prototype of the PIR with inflated clamps for attach-to-pipe pose.

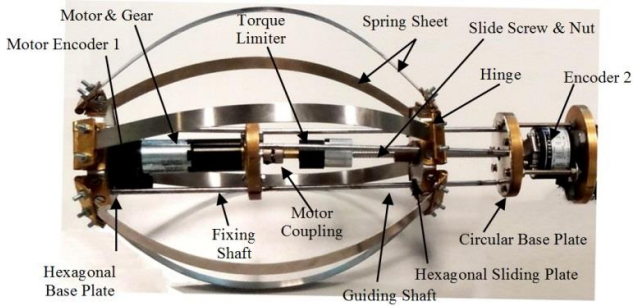


Fig. 3a. Components of a “Clamp”.

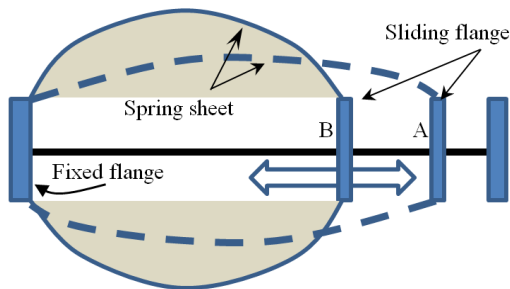


Fig. 3b. When slide flange moves from A to B, a wider radial dimension for the clamp can be achieved.

However, since the robot is designed to move through pipes of different diameters and/or, through a pipe of changing diameter, this maximum clamping force can be chosen to be constant regardless of the pipe diameter by installing a mechanical torque limiter between the power screw and the motor (Fig. 3a). When the torque limiter is engaged, i.e., the torque on the shaft is less than a preset value that depends on its specifications, the motor and the power screw will be in direct drive. Once the motor torque exceeds the limiter’s preset torque value, the torque limiter disengages and disconnects the motor from the power screw causing the motor to continue spinning but not the power screw. Therefore, the hexagonal flange that slides along the power screw will stop at a certain distance along the power screw causing the spring sheets to apply a constant clamping force to the pipe without the need to know the diameter of the hosting pipe, and will set the clamping force at its maximum value.

The controller, in turn, receives two encoder readings, one from motor encoder 1 and the second is from encoder 2 that is installed at the end of the power screw (Fig. 3a). When the motor is engaged with the power screw, both encoders will read the same angular velocity, but once disconnected, the angular velocity of the power screw encoder will drop to “zero” thus, the controller realizes that the clamp is tightened with its maximum force to the pipe and ends the “clamping task” and starts the “move task”.

Another feature of the clamp is the hole-finding sensor assembly which is mounted on the frontal clamp (Figs. 2 and 4). The sensor assembly is designed to identify the existence of obstacles and/or to realize the clear path during the robot’s movement especially when the robot passes through an elbow, or through local variations like a step change in pipe diameter, eccentric sections, or connection into a network of pipes through T-junctions.

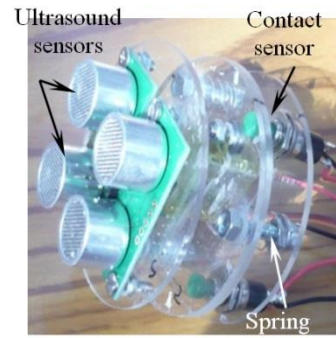


Fig. 4. Ultrasound assembly set for hole- finding feature

The path-finding sensor assembly (Fig. 4) consists of three parallel circular discs with an ultrasonic sensor placed on the top disc, with the base plate attached to the nose of the frontal clamp. Using a micro servo-motor, the top disc spins 270 degrees clockwise and counter-clockwise searching for a clear path while the robot is in motion. The other two discs are separated by 3 helical springs separated by 120 degrees to keep the plates parallel, and each is concentric with a contact sensor to detect any compression in the spring if it occurs. If the robot fails to realize the clear path by the ultrasonic sensors, signals from the contact sensors when the robot nose hits an obstacle will guide the middle segment to steer the robot to the appropriate path.

*B. Middle Segment*

This segment (Figs. 1 and 2) is responsible for two important tasks, propulsion and steering. As shown in Fig. 5a, it consists of three polymeric rods connected from one end to universal joints which are fixed to an end flange, while at the other end, the nylon rods connects to aluminum blocks that can travel along motor-driven power screws. When the blocks travel along the power screws, the nylon rods can extend and retract, causing the middle segment to push/pull its end flange along the robot’s length (Fig.5a). When the driving micro-motors spin with the same speed, the nylon rods extend or retract with the same linear rate which pushes/pulls the end flange along a linear path. This enables the robot, with the aid of the clamping segments to propel along a linear path. On the other hand, if one of the rods extends faster than the other two, the nylon rod bends causing the end flange to steer (Fig. 5b). Hence, the middle module enables the robot to propel and to steer to the desired direction as instructed by the controller based on the direction feedback obtained from the sensor assembly.

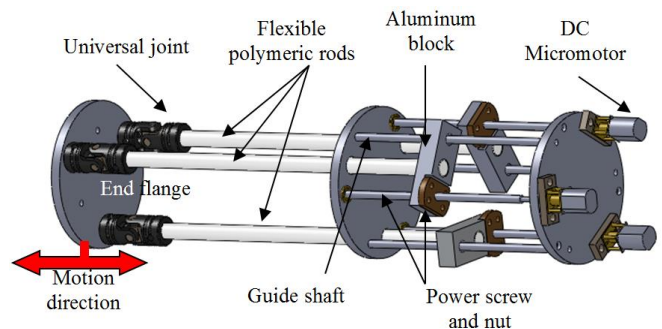


Fig. 5a. Middle segment’s details



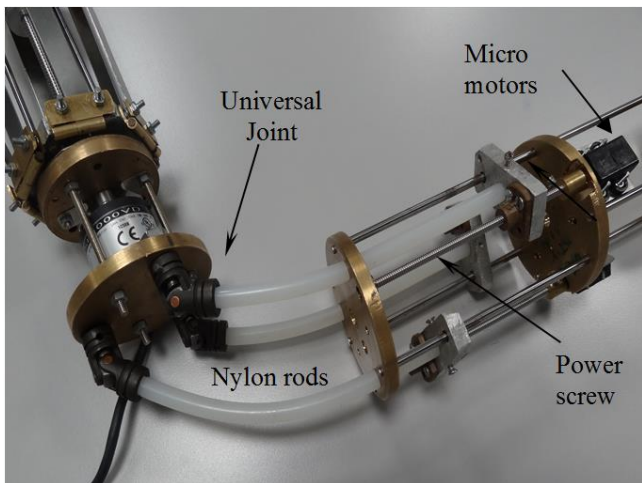


Fig. 5b. Robot can steer up to 90 degrees.

It is worth mentioning that the nylon rods are selected to be strong enough to support the weight of the robot clamps and provide sturdiness to the robot structure, but should be flexible to allow bending when steering is needed. Polyurethane rods were used since its properties meet such requirements.

### C. Motion Sequence and Pattern

The three modules of the robot (two end clamps and middle segment) go through the following sequential movement pattern that causes the robot to propel by an inch-worm motion.

Initially, the front and rear clamps are in attach-to-pipe pose where their spring sheets stick to the inner walls of the pipe, while the middle module nylon rods are extended (Fig. 6a). The motion starts by relaxing the rear clamp from the pipe (Fig. 6b). This can be done by relaxing the spring sheets of the clamp using the clamp's power screw. Then the nylon rods of the middle segment shrink/retract causing the rear clamp to move forward (Fig. 6c). Once the rods are fully extended, the rear clamp attaches to the pipe walls again (Fig. 6d). Next, the front clamp releases the pipe (Fig. 6e) and the nylon rods of the middle module extend, i.e. protrude, pushing the front clamp forward (Fig. 6f). Once the nylon rods are fully extended, the rear clamp is set to attach to the pipe walls again (Fig. 6g).

Repeating that motion pattern can cause the robot to propel in one direction while reversing the sequence can reverse the motion direction.

## III. MATH TESTS AND RESULTS

### A. Motion in straight pipe segment

In order to determine the capability of moving along a linear path, the robot was tested inside a 15 mm ID Plexiglas pipe. The clamping force and propulsion speed depend on the robot parameters and specifications of the components used to build it as explained in this section.

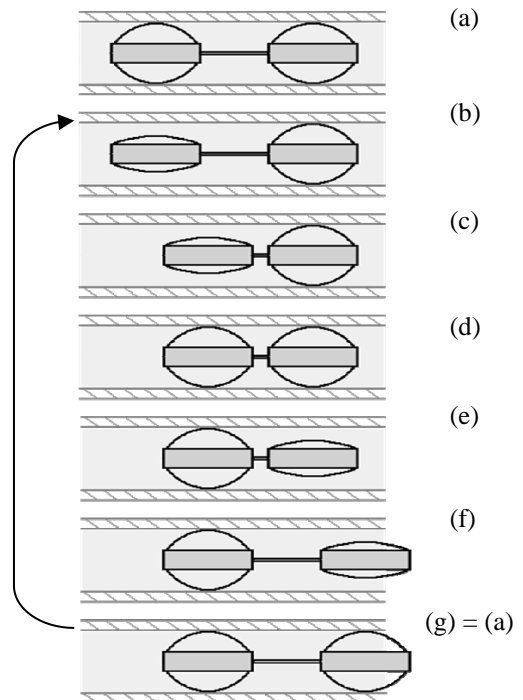


Fig. 6. Motion sequence of the robot adopts inch-worm motion pattern

## IV. UNITS

However, in order for the robot to be able to travel vertically through a pipe, the weight of the robot must be less than the minimum of either the clamping force of a single clamp or the drag force generated by the middle segment, whichever is less. Therefore, those forces were measured as follows:

To measure the clamping force, the clamps were attached to the pipe with maximum force which is dependent on the torque limiter's capacity as mentioned earlier, then the robot nose was hooked to a load cell and pulled by a test motor by gradually increasing the motor torque while monitoring the position of the robot inside the pipe. The clamping force was measured by the load cell as the force sufficient to slide the robot. The experimental setup used to conduct the test is shown in (Fig. 7a) and explained further in the illustrative diagram of Fig. 7b.

Also the same setup was used to measure the drag force. For this, the test motor brake was engaged and one of the clamps is set free while the other is clamped to the pipe, and the drag force was measured by the load cell as the maximum pulling force caused by the middle segment without slippage of the attached clamp. (Fig. 7c). Test results showed that, for its current configuration, the robot clamps together can provide a 76 N, i.e., 38 N/clamp, while the drag force was found to be 83N. It is obvious that the critical force to compare with the robot's payload in the case of climbing a vertical pipe is the clamping force. Since the weight of the robot, 3.55 kg = 34.8 N is less than the clamping force, the robot could travel vertically through the pipe. Note that the roughness of the inner surface of the pipe will affect these values because it affects both the clamping and the drag

forces. Also note that the drag and clamping forces that suffice travelling through a vertical pipe will be adequate to enable travelling through a horizontal pipe.

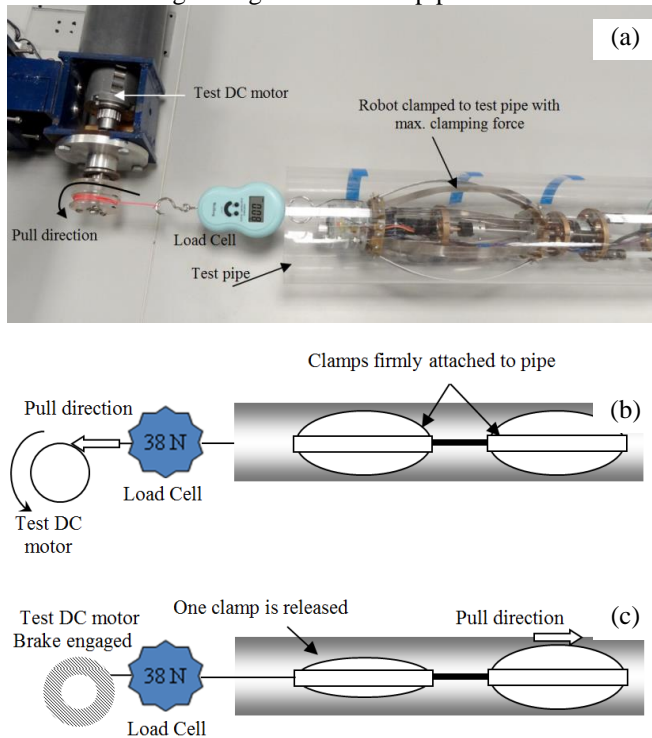


Fig. 7. (a) Test bed used for clamping force measurement (b) Clamping force measurement, (c) Drag force measurement.

Moreover, the clamping force to the walls can be adjusted or changed by changing one or more of the following parameters/specifications: 1) the spring sheets' thickness, width and/or material; 2) the torque limiter's set-torque. The robot's current configuration uses 0.63 mm thick x 10 mm wide stainless steel spring sheets, and the selected torque limiter's capacity is 392 mN·m. Furthermore, the length of the spring sheets controls the robot's capability to handle larger pipe diameters. Fig. 8 shows the increase in the contact surface between the spring sheets of the clamp and the pipe surface as a result of using a torque limiter of higher capacity.

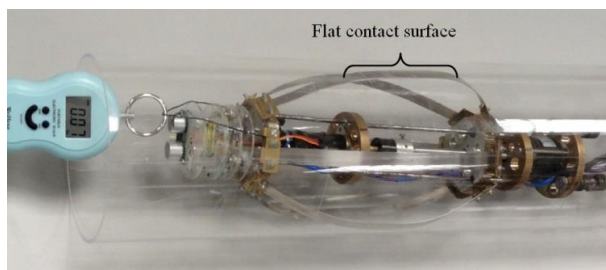


Fig. 8. Flat spring sheet with larger surface of contact with the pipe results from using a torque limiter of larger capacity.

The propulsion speed was calculated based on the total time required to complete the full cycle of an inch-worm motion pattern as described in the previous section and found to be 2 mm/s. However, the speed can be improved by minimizing the controller's wasted time. For instance, attaching/releasing the clamps to the pipe can be performed by spinning the clamp motor few spins sufficient to apply release the necessary force or to release the clamp instead of completely flattening the spring sheets. Also, this speed can be improved further by using micro-motors with higher RPM to drive the elastic rods of the middle segment and/or by selecting power screws with larger pitch or lead. Also power transmission gears will be considered in future versions.

Table I summarizes the specifications of the robot based on its current configuration.

Table I. Specifications of the Robot.

Requirement considered	Specification
Weight	< 3.6 kg
Material	Brass and aluminum
Architecture	Modular: Clamp- steering/propulsion segment- Clamp
Motion type	Inch-worm
No. of Actuators	5
Power supply	Self-powered , 8-AA batteries+ 2X 9V batteries
Dimensions:	(Length)
	(Outer diameter)
	109 cm (fully retracted)
	117.5 cm (fully extended)
	(min) 6.5 cm- fully collapsed clamps
	(max) 22 cm- fully expanded clamps
Max linear stroke	8.5 cm
Linear propulsion speed (tested in 15 cm ID pipe)	2 mm/s
Clamping force (tested in a 15 cm ID Plexiglas pipe )	76 N
Max turning angle	90 degrees
Operating mode	Autonomous

### B. Motion in turns

The motion pattern can be briefed as follows: the middle module is responsible for pushing the front of the robot, to steer it, and to drag the rear section forward by active actuators. However, the rear section comprises two passive ball joints (Figs. 1 and 2) to allow the robot body to bend when passing through turns. Fig. 9 shows the robot immersing from a straight pipe to pass through an elbow during experimental test of the capability of the robot to handle turns. For this experiment, a pipe/elbow diameter of  $D_p=180$  mm and an elbow radius  $r_e=270$  mm where used (in urban gas pipelines,  $r_e$  is usually  $1.5 D_p$ ).

Pipeline configurations and dimensions impose geometrical constraints on the robot dimensions. S Roh and H Choi provided detailed analysis on such restrictions [12]. The analysis for the proposed robot provided in this section is based on their approach.

Since the robot comprises a series of rigid bodies, the analysis will consider the longest rigid part which, if passes the elbow, all other parts can pass successfully. Referring to Fig. 2, our target part is the frontal clamp that includes the

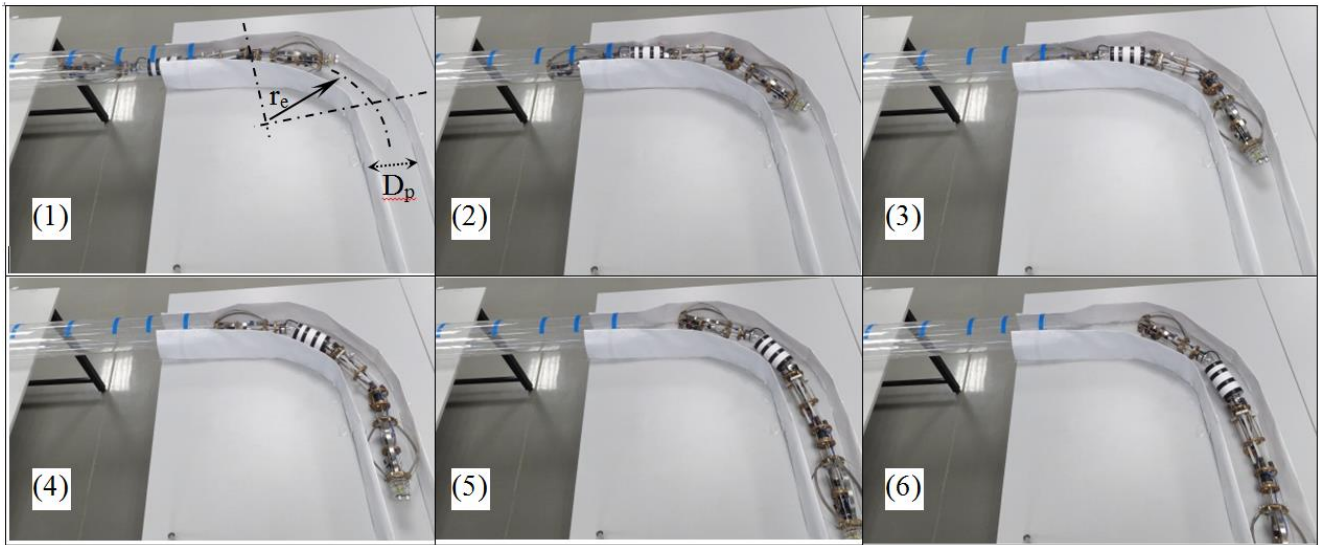


Fig. 9. Robot emerging from a straight pipe then passing through an elbow,  $D_p=180$  mm,  $r_e=1.5D_p= 270$  mm

sensor assembly with a total length of 340 mm. The worst scenario is when the part makes  $45^\circ$  with the tangent to the elbow as shown in Fig. 10.

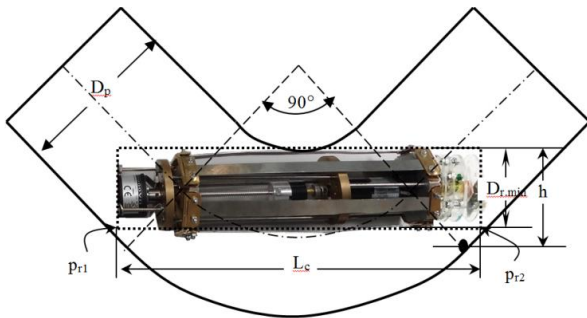


Fig. 10. Collapsed Clamp inside an elbow.  $D_{r,min}= 65$ mm.

From the geometry, the length of the robot's longest rigid part  $L_c$  is given as follows: in case the length exceeds the distance  $\overline{p_{r1}} - \overline{p_{r2}}$ , the robot's min. diameter  $D_{r,min}$  has the range of

$$0 < D_{r,min} \leq \left[ \frac{\sqrt{2}}{2} \left( r_e + \frac{D_p}{2} \right) - \left( r_e - \frac{D_p}{2} \right) \right] \quad (1)$$

where  $r_e$  is the radius of the elbow from center to its middle, and  $D_p$  is the pipe diameter.

The length of the robot is given by

$$L_c = 2\sqrt{2} \left[ r_e + \frac{D_p}{2} - \frac{\sqrt{2}}{2} \left( D_{r,min} + r_e - \frac{D_p}{2} \right) \right] \quad (2)$$

setting  $r_e = 1.5D_p$ , then

$$0 < D_{r,min} \leq 0.414 D_p \quad (3)$$

Considering this range of  $D_{r,min}$  from (3) in (1)

$$2\sqrt{2} D_p \leq L_c < 3.66 D_p \quad (4)$$

The second case is when the length of the longest rigid body is within the elbow curvature, i.e. the length is less than the distance  $\overline{p_{r1}} - \overline{p_{r2}}$ , then

$$\left[ \frac{\sqrt{2}}{2} \left( r_e + \frac{D_p}{2} \right) - \left( r_e - \frac{D_p}{2} \right) \right] < D_{r,min} < D_p \quad (5)$$

$$\text{and } L_c = 2 \cdot \sqrt{\left[ \left( r_e + \frac{D_p}{2} \right)^2 - \left( D_{r,min} + r_e - \frac{D_p}{2} \right)^2 \right]} \quad (6)$$

again, when setting  $r_e = 1.5D_p$  and considering the range of  $D_{r,min}$  given in (5),

$$(\sqrt{2} - 1)D_p < D_{r,min} < D_p \quad (7)$$

$$0 < L_c < 2\sqrt{2} D_p \quad (8)$$

The preceding analysis assumes that the robot's radial dimension  $D_{r,min}$  is slightly smaller than the height  $h$ . From the equations, it is obvious that if  $L_c$  satisfies (8), then the robot can pass through straight segments and elbows, provided that the robot's configuration can handle the pipe diameter.

Therefore, the maximum pipe diameter depends on the 1) radial dimension that the robot's configuration can handle, and; 2) that the robot's  $D_{r,min}$  and  $L_c$  satisfy the constraints imposed by (7) and (8). However, (8) confirms that the range of  $L_c$  that can pass an elbow of  $D_p=180$  mm, which was used for the test elbow, is  $0 < L_c < 509$ , and this range includes  $L_c=340$  mm (that is the longest rigid body in our robot). Note that the robot's configuration can handle pipe diameters between 65-220 mm, which includes the 180 mm pipe/elbow diameter.

One of the main advantages of the proposed robot would be obvious when passing through bends as the flexible spring sheets can take the shape of the hosting pipe when clamping to the pipe.



V. CONCLUSION

A novel in-pipe inspection robot has been designed and constructed. The robot's features enable it to navigate autonomously through a pipeline. The robot that is configured with three main modules, two clamps and one drive segment adopts inch-worm motion pattern. Its clamping modules enable the robot to dynamically adjust its radial dimension between 65-220 mm, and clamping force to attach to pipes of different inner diameters and overcome the obstacles associated with changes in pipe diameters, thus it can travel through pipelines that comprise segments of varying inner diameters. It comprises a sophisticated middle module that enables it to propel, and to steer into the desired direction when approaching an elbow or a junction. In addition, the robot is equipped with a hole-finding sensor assembly that allows it to realize the clear path along turns and T-junctions.

REFERENCES

- [1] N. Saga, T. Nakamura, "Development of a peristaltic crawling robot using magnetic fluid on the basis of the locomotion mechanism of the earthworm", *Smart Materials and Structures*, 2004,13, pp.566-569.
- [2] F. Kirchner and J. Hertzberg "A Prototype Study of an Autonomous Robot Platform for Sewerage System", *Maintenance Autonomous Robots*, 1997; 4(4), p. 319-331.
- [3] HB. Kuntze and H. Haffner, "Experiences with the development of a robot for smart multisensoric pipe inspection", *Proc. IEEE International Conf. on Robotic and Automation*, 1998. p. 1773-8.
- [4] SG Roh and HR Choi, "Differential-drive in-pipe robot for moving inside urban gas pipelines", *IEEE Transactions on Robotics*, 2005; 21(1), pp. 1-17.
- [5] M. Muramatsu, N. Namiki and R. Koyama, "Autonomous mobile robot in pipe for piping operations", *Proc. IEEE/RSJ International Conf. on Intelligent Robots and Systems*, 2000. pp. 2166-71.
- [6] M. Moghaddam and M. R. Tafti, "Design, modeling and prototyping of a pipe inspection robot", 22<sup>nd</sup> Int. Symp. on Automation and Robotics in Construction (ISARC), 2005.
- [7] Yunwei Zhang, and Guozheng Yan, "In-pipe inspection robot with active pipe-diameter adaptability and automatic tractive force adjusting", *Mechanism and Machine Theory*, 2007, 42, pp. 1618-1631.
- [8] HR. Choi and SM. Ryew "Robotic system with active steering capability for internal inspection of urban gas pipelines", *Mechatronics*, 2002; 16(12), pp. 713-36.
- [9] Z. Zhu and Z. Pan, "Miniature pipe robots", *Industrial Robot: An International Journal*, 2003; 30(6), pp. 575-83.
- [10] I. Hayashi, N. Iwatsuki, K. Morikawa and M. Ogata, "An in-pipe operation microrobot based on the principle of screw", *International Symposium on Micromechatronics and Human Science*, 1997, pp. 125-9.
- [11] M. Horodincea, I. Dorftel, E. Mignon and A. Preumont, "A simple architecture for in-pipe inspection robots", *Proc. International Colloquium on Mobile and Autonomous Systems*, 2002, pp. 61-4.
- [12] S. Roh and H. R. Choi, "Differential-drive in-pipe robot for moving inside urban gas pipelines", *IEEE Transactions on Robotics*, 2005, 21(1), pp 1-17.
- [13] J. Park, T. Kim, H. Yang, "Development of an actively adaptable in-pipe robot", *Proc. IEEE International Conference on Mechatronics (ICM)*, 2009.
- [14] K. Suzumori, T. Miyagawa, M. Kimura, Y. Hasegawa, "Micro Inspection Robot for 1-in Pipes", *IEEE/ASME Transactions on Mechatronics*, 4(3), 1999, pp.286-292.
- [15] S. Hirose, H. Ohno, T. Mitsui and K. Suyama, "Design of In-Pipe Inspection Vehicles for  $\phi 25$ ,  $\phi 50$ ,  $\phi 150$  Pipes", *Journal of Robotics and Mechatronics*, 12(3), 2000, pp. 310-317.
- [16] T. Fukuda, H. Hosokai, M. Uemura, "Rubber gas actuator driven by hydrogen storage alloy for in-pipe inspection mobile robot with flexible structure", *Proc. IEEE International Conf. on Robotics and Automation*, 1989, p. 1847-52.
- [17] S. Aoshima, T. Tsujimura and Yabuta "A miniature mobile robot using piezo vibration for mobility in a thin tube", *Transactions of ASME, Journal of Dynamic Systems, Measurements and Control*, 1993, 115, p. 270-8.
- [18] C. Anthierens, A. Ciftci and M. Betemps, "Design of an electro pneumatic micro robot for in-pipe inspection", *Proc. IEEE International Symposium on Industrial Electronics*, 2, 1999, pp. 968-72.
- [19] KU. Scholl, V. Kepplin, K. Berns and R. Dillmann, "Controlling a multi-joint robot for autonomous sewer inspection", *Proc. IEEE International Conf. on Robotics and Automation*, 2000, 2, p. 1701-6.
- [20] S. Wakimoto, J. Nakajima and M. Takata, "A micro snake-like robot for small pipe inspection. *Proc. International Symposium on Micro Mechatronics and Human Science*, 2003, pp. 303-8.
- [21] J. Borenstein, G. Granosik and M. Hansen, "The OmniTread serpentine robot for industrial inspection and surveillance", *International Journal on Industrial Robots, Special Issue on Mobile Robots*, 2005, 32(2), pp.139-48.
- [22] A. Zagler and F. Pfeiffer, "MORITZ" a pipe crawler for tube junctions". *Proc. IEEE International Conf. on Robotics and Automation*, 2003, pp. 2954-60.
- [23] W. Neubauer, "A spider-like robot that climbs vertically in ducts or pipes", *Proc. IEEE/RSJ International Conference on Intelligent Robots and Systems*, 1994, pp. 1178-85.
- [24] W. Fischer, F. Tâche, and R. Siegwart, "Inspection system for very thin and fragile surfaces, based on a pair of wall climbing robots with magnetic wheels," in *Proc. IEEE/RSJ Int. Conf. Intelligent Robots and Systems*, San Diego, CA, USA, 2007, pp. 1216-1221.
- [25] Basem F. Yousef, et. al., "IN-PIPE INSPECTION ROBOT". In *Proc. of the 15<sup>th</sup> Int. Conf. on Climbing and Walking Robots and the Support Technologies for Mobile Machines*, BA, USA, 2012, pp. 289-296.